Chapter 3 – Structural characterization of triazines.

As stated in the previous chapter, the characterization of the synthesized triazine products by NMR spectroscopy was difficult, on one side because of their low solubility in most common deuterated solvents ($CDCl_3$, DMSO-d_6, DMF-d_6 or MeOD-d_3) at room temperature, and on the other hand because of the complexity of their spectra.

In the case of the bis-amino substituted triazines low solubility was the major issue. It was hypothesized that intermolecular hydrogen bonding and π-stacking between aromatic moieties could generate tight linkages between molecules,[123] which would lead to the formation of insoluble aggregates.

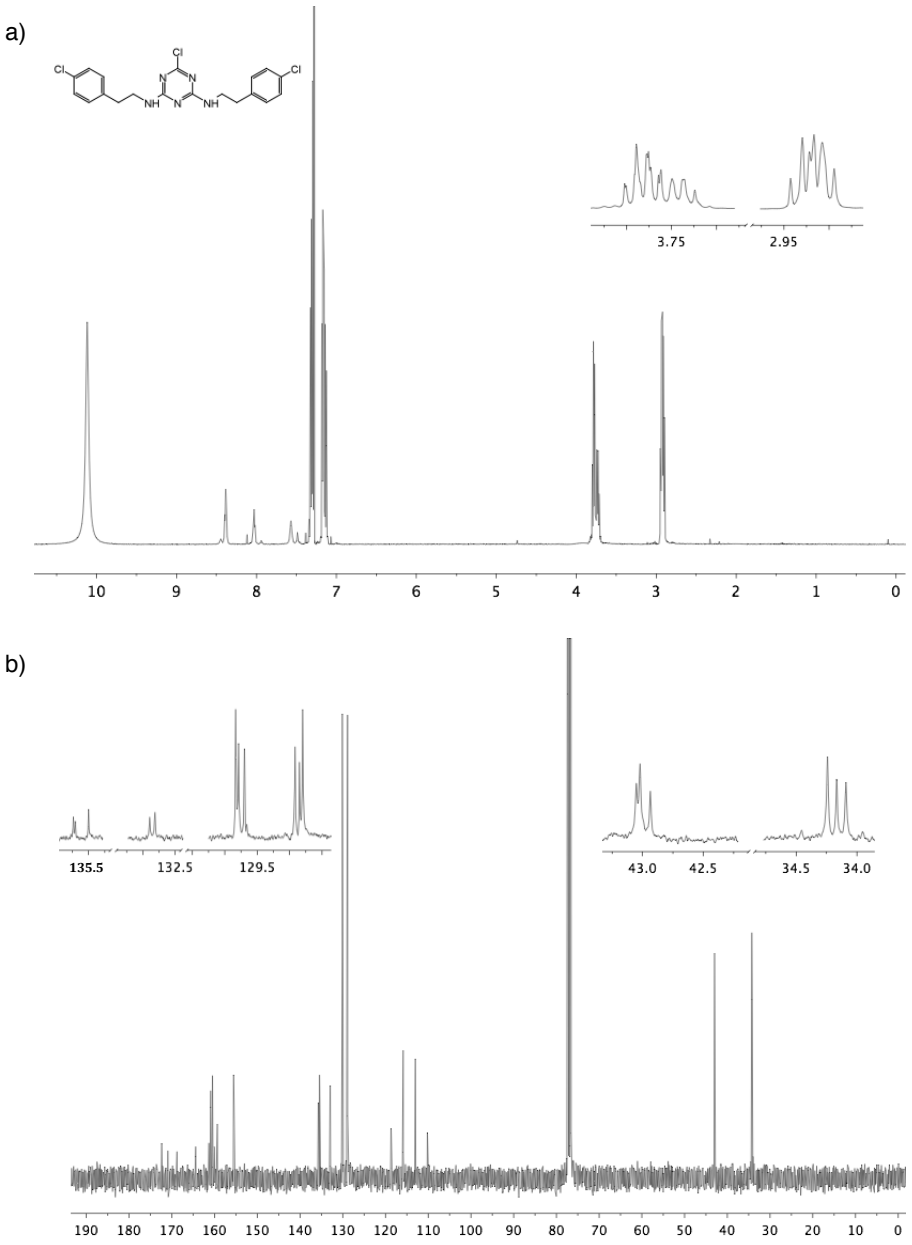

Figure 64. a) ^{1}H-NMR and b) ^{13}C-NMR spectra of triazine **22** in $CDCl_3$, 7% TFA (v/v). Insets show regions where signals split into several peaks or complex signals.

Therefore, it was reasoned that using TFA as cosolvent of the NMR samples would favor the protonation of the triazines, reducing their capacity to establish hydrogen-bond and π-stacking interactions between aromatic moieties. Thus, it was found that using a mixture of $CDCl_3$ with 7% TFA at room temperature was adequate to solubilize most bis- and tris-aminosubstituted triazines. Similarly, using $CDCl_3$ at ~50 ºC as solvent of the NMR samples allowed in some cases the acquisition of spectra without the need of using TFA. However, the use of TFA and/or high temperature led in some cases (e.g. triazines **71** and **72**) to the decomposition of the sample. Other deuterated solvents that were used for specific samples were d_3-acetonitrile or d_5-pyridine. Still, the improvements in solubility did not change the complexity of the spectra. Figure 64 shows the ^{1}H- and ^{13}C-NMR spectra of triazine **22**, illustrating the high apparent multiplicity of the signals that correspond to the protons of the aliphatic moieties of the triazine and the splitting in several peaks of the signals corresponding to most carbon atoms. The fact that this complexity could not be reduced after additional purification attempts led us to consider that a dynamic equilibrium could be taking place in solution.

It is well known that aminosubstituted-1,3,5-triazines can exist as mixtures of rotamers in conformational equilibrium.[123-126] This dynamic equilibrium originates on the restricted rotation of the bonds between the triazine ring and the amino substituents. Due to resonance, different resonant canonical structures can be drawn where the amine nitrogen attached to the triazine ring has sp^2 hybridisation (Figure 65a), leading to a net stabilization of the planar conformation. Rotation about the triazine-amino bond decreases the sp^2 character of the amine nitrogen atom until it becomes purely sp^3, with its consequent piramidalisation and loss of stabilization, thus giving rise to the rotation barrier.[124] If this barrier is high enough it will result on the generation of different rotamers which interconvert slowly in the NMR time scale, generating multiple peaks for some nuclei on the spectrum. The number of conformers will depend on the molecular symmetry: three conformers for symmetrically disubstituted triazines (Figure 65b) and four for trisubstituted ones (Figure 65c).

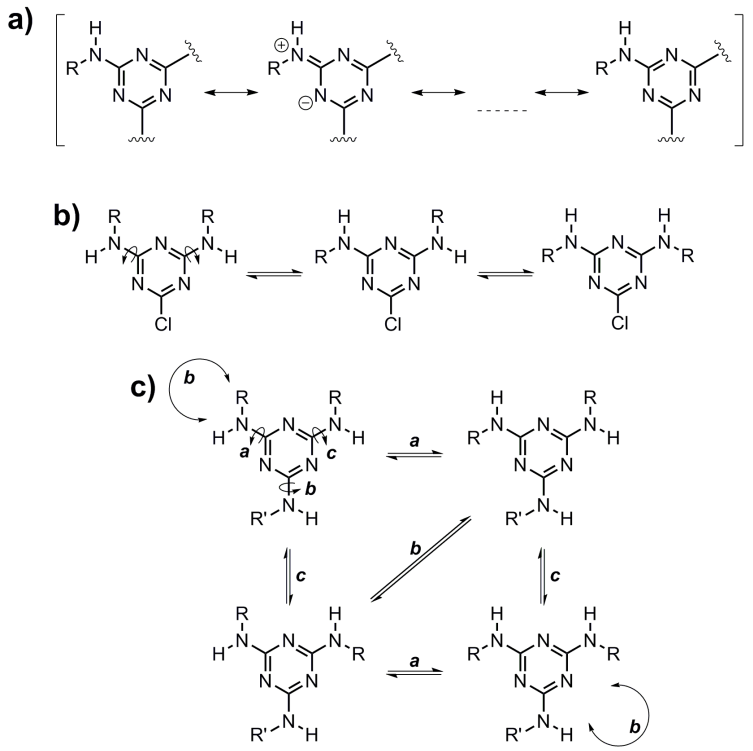

Figure 65. a) Resonance structures for the amine side chains of amino substituted triazines. Conformational equilibria due to single rotations of amine-triazine bonds in the (b) bis- and (c) tris-amino substituted triazines under investigation.

The ^{1}H- and ^{13}C-NMR spectra of all compounds can be found in annex 5 the attached CD.

3.1 Full NMR characterization of selected tris-aminosubstituted triazines.

Tris-aminosubstituted triazines exhibited an improved solubility in comparison with bis-substituted ones, however their spectra were more complex since they had, at least, one more possible rotamer in equilibrium.

Figure 66 shows the ^{1}H-NMR spectrum of triazine **46** which illustrates this complexity: every signal appears as a broad multiplet, except the singlet at 2.80 ppm that can be attributed to the dimethylamino group. The broad multiplets between 3.66-2.82 ppm and the one at 1.98 ppm correspond to the methylene protons of all the species in equilibrium.

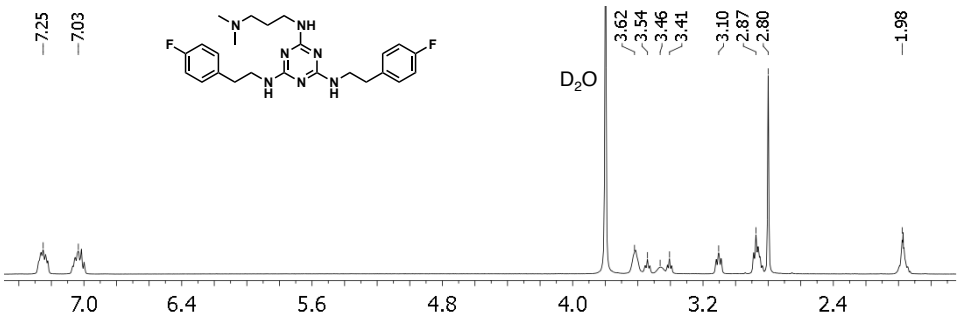

Figure 66. ^{1}H-NMR spectrum of triazine **46** in CD_3CN/D_2O/TFA (86:7:7) at 25 ºC.

The homocorrelation spectrum (DQCOSY) of **46** reveals three spin systems (Figure 67). The first one includes the signals with chemical shifts at 1.98, 3.10 and 3.50-3.37 and corresponds to the propylamine moiety. Crosscorrelation peaks between signals at 3.10 ppm and 3.50-3.37 ppm are smaller than those with the signal at 1.98 ppm, indicating that the last one can be assigned to the central methylene group while the other two belong to both methylenes at the extremes of the propyl chain.

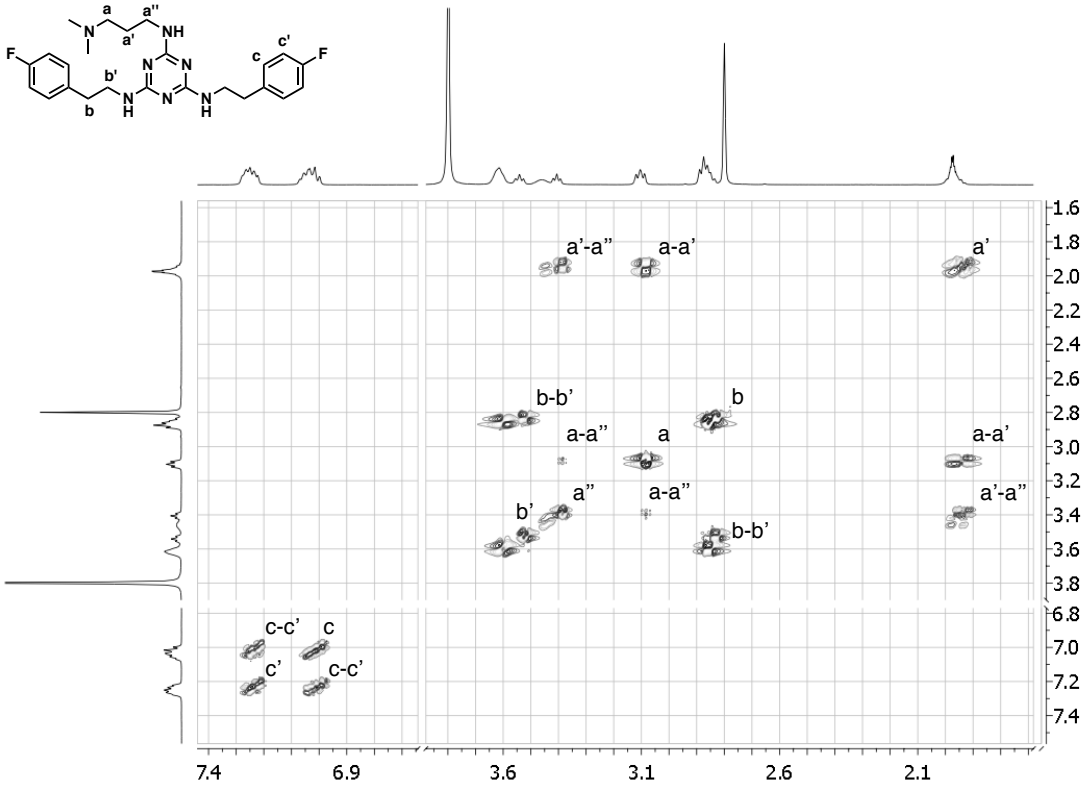

Figure 67. 2D gDQCOSY spectrum of triazine **46** in CD_3CN/D_2O/TFA (86:7:7). Correlated spin systems are named with the letters of the correlated signals from the diagonal.

A second system containing signals with chemical shifts at 2.87 and .66-3.51 ppm can be related to the alkylic chain of the 4-fluorophenethylamino moieties. Finally,

the system formed by the complex signals centered at 7.03 and 7.25 ppm corresponds to the aromatic protons of the two fluorophenyl groups.The 2D NOESY experiment completed the ^{1}H-NMR characterization of product **46** by correlating signals of protons which are close in space (Figure 68). In addition to interactions through space, NOESY experiments can detect chemical exchange. In this respect, the two pairs of multiplets between 3.66-3.50 and 3.50-3.37 ppm show crosscorrelation peaks between each pair with the same phase as the diagonal, indicating that a polarization transfer (pt) mechanism is occurring due to the exchange between rotamers in equilibrium. Looking at the signals from the dimethylaminopropyl moiety, it can be observed that the singlet at 2.80 ppm, assigned to the dimethylamino group, shows correlation with the signals centered at 1.98 and 3.10 ppm but not with the broad signals between 3.50-3.37 ppm.

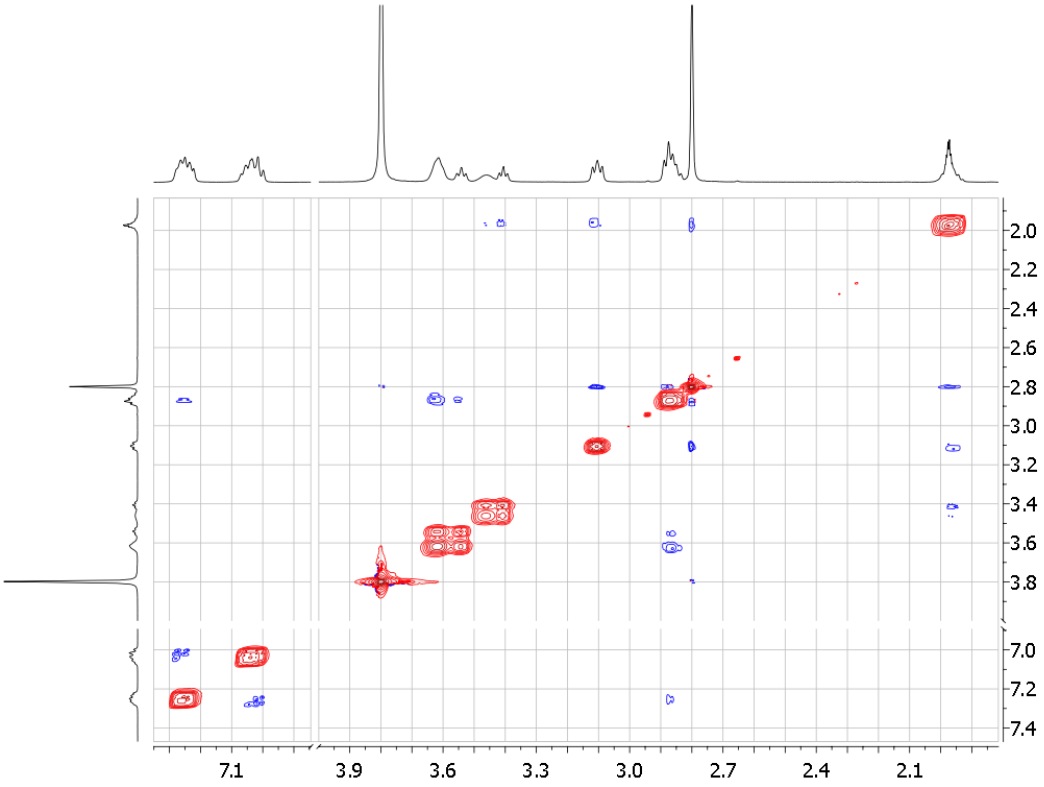

Figure 68. 2D-NOESY spectrum of triazine **46** in CD_3CN/D_2O/TFA (86:7:7) showing phase and anti-phase signals.

This confirms that these last ones belong to the methylene which is farther apart from the dimethylamino group, i.e. the methylene closer to the triazine ring, while the other two correspond to the central and third methylenes of the propyl chain, respectively. On the other hand, there is also a correlation between the signals at 3.66-3.50 and that centered at 2.87 ppm, which were already assigned to the methylenes of

the phenethyl moieties. Lastly, the signals at 7.03 and 7.25 ppm, that arise from the aromatic protons of the 4-fluorophenyl groups, show crosscorrelation peaks between them, and the second one also with the broad signal at 2.87 ppm, allowing to assign this system to the $\underline{H}C_{Ar}C_{Ar}C\underline{H_2}$ moiety of the phenethylamino groups, and the complex system at 3.66-3.50 to the protons of the amine-bound methylene in rotamer exchange.

Concerning the ^{13}C-NMR spectrum of triazine **46** (Figure 69), it also displayed a relatively high complexity due to the appearance of several peaks that arose from the dynamic equilibrium between conformers. In addition, coupling of the aromatic carbon nuclei to the 4-fluoro substituent was also observed.

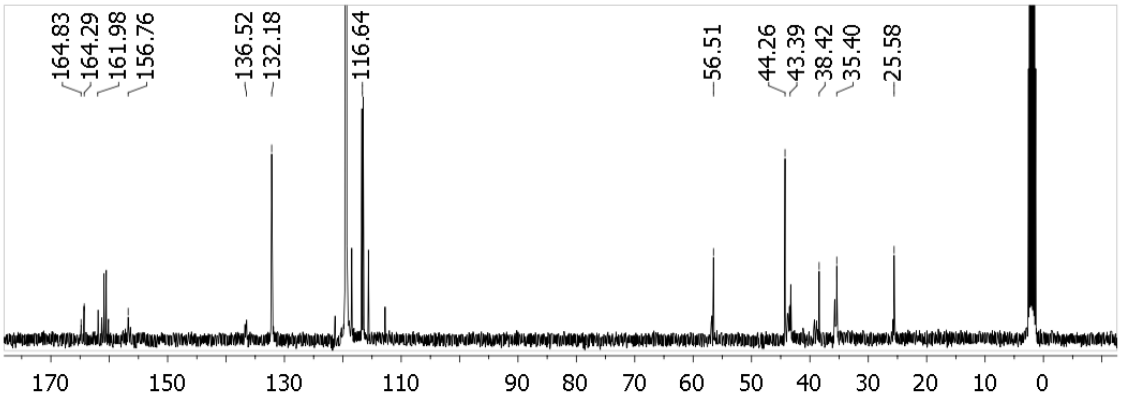

Figure 69. ^{13}C-NMR spectrum of triazine **46** in CD_3CN/D_2O/TFA (86:7:7) at 25 ºC.

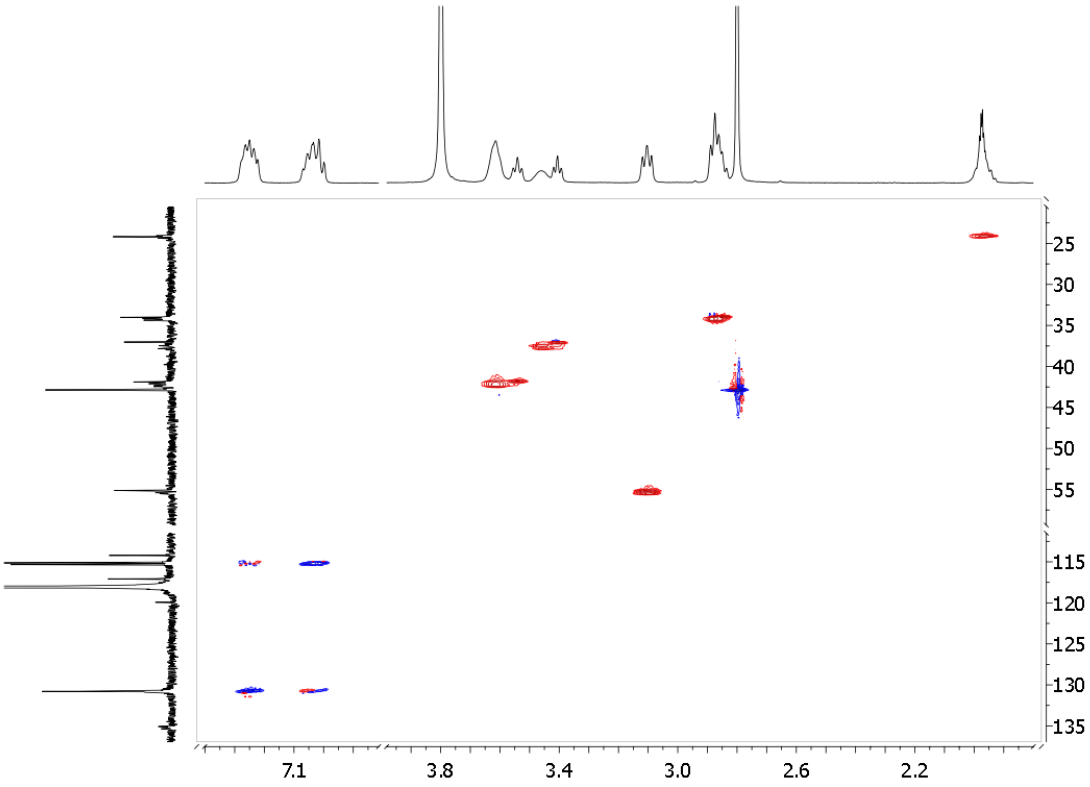

Figure 70. gHSQC spectrum of triazine **46** in CD_3CN/D_2O/TFA (86:7:7).

Having previously assigned all the signals on the ^{1}H-NMR spectrum, the bidimensional ^{1}H-,^{13}C-gHSQC experiment (Figure 70) allowed the unequivocal assignment of most of the signals of the ^{13}C-NMR spectrum of **46**, thus confirming its structure.

Another example of a product with complex NMR spectra was compound **43**. This triazine contains an *N*-methylpiperazino moiety in its structure and, although it is essentially symmetric, its ^{1}H-NMR spectrum revealed again a high complexity. The piperazine ring introduces additional possible conformations where protons on the same carbon become magnetically non-equivalent (Figure 71).

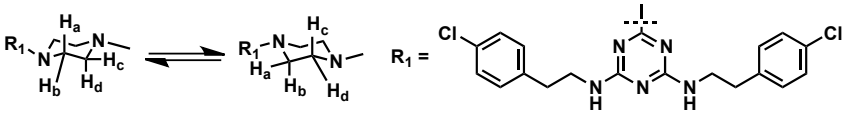

Figure 71. Chair-chair equilibrium of the piperazine ring of triazine **43**.

To study the conformational exchange and space proximity between protons in the structure of **43**, 1D-NOESY experiments were performed (Figure 72).

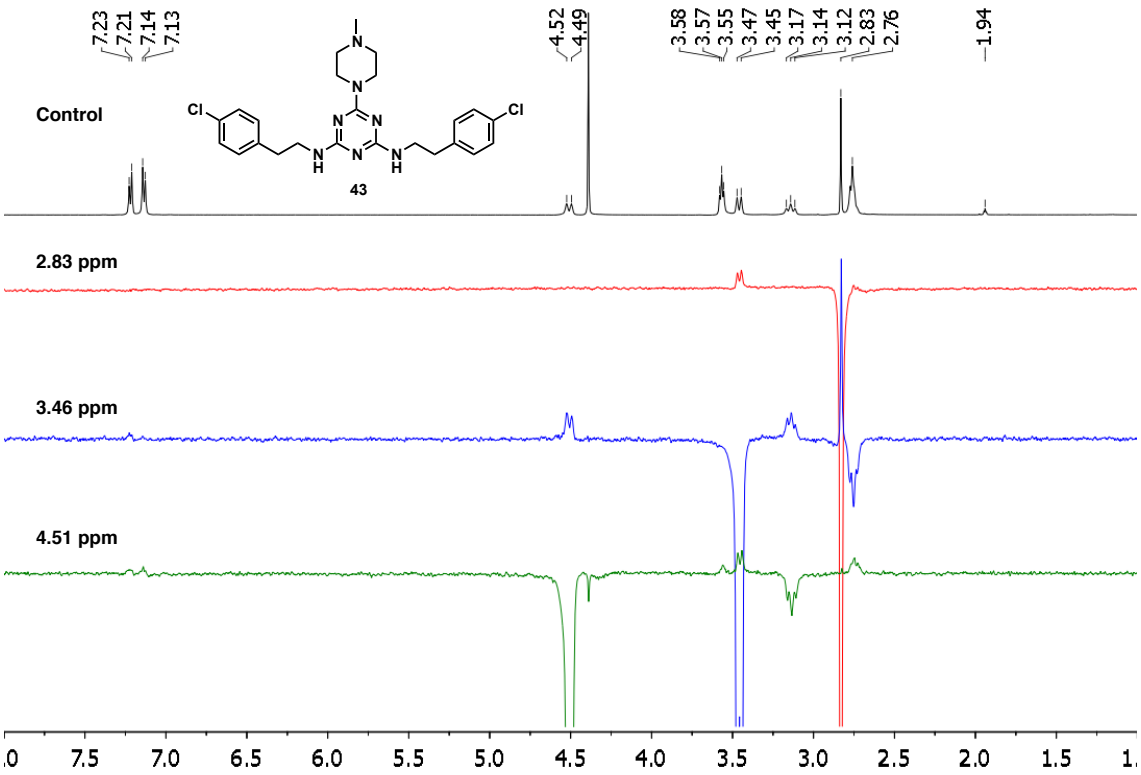

Figure 72. ^{1}H-NMR in ACN-d_3 (25 ºC) and 1D-NOESY experiments for product **43**. Irradiated frecuencies (in ppm) are shown at the left of the spectra.

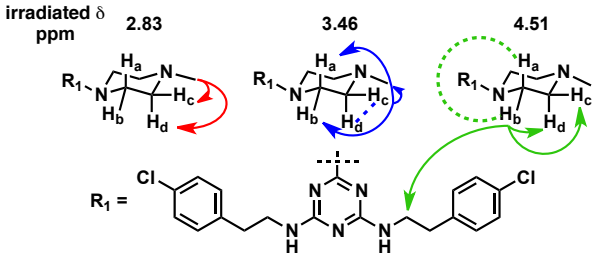

Figure 73. Observed correlations from the 1D-NOESY experiments shown in Figure 72. Dotted lines represent a signal with the same phase than the decoupled signal while continuous arrows represent an opposite phase signal.

Signals centered at 4.51, 3.46, 3.14 and part of the signal at 2.76 ppm belong to the protons of the piperazine ring, while the singlet at 2.83 ppm corresponds to the methyl bound to the piperazine nitrogen. This assignment was based on the following observations. Exchange between the equatorial and axial protons of the piperazine results on polarization transfer, which is observed when the decoupler was set at 3.46 (pt to the signal at 2.76 ppm) and 4.51 ppm (pt to the signal at 3.14 ppm). Thus, signals at 3.46 and 2.76 ppm must belong to the enantiotopic protons of the methylenes (C3'/C5') bound to the methylamino group of the piperazine, since they show exchange (blue trace, Figure 73) and a positive NOE effect on irradiation at 2.83 ppm. On the other hand, since irradiating at 3.46 ppm results on positive NOE effects on signals at 4.51 and 3.14, and irradiating at 4.51 ppm elicits positive NOE on the signals at 3.46 and 2.76 ppm, it was concluded that signals at 4.51 and 3.14 must belong to the protons of the other two methylenes (C2'/C6') of the piperazine. Finally, the broad signals at 3.57 and part of the signal at 2.76 ppm, overlapped with some of the above signals from the piperazine, belong to the methylenes of the phenethylamino moieties.

Further confirmation of these assignments was obtained from analysis of the gDQCOSY spectrum (Figure 74). Here, it can be observed that the triplet-shaped signal at 3.57 ppm only correlates with the overlapped signal at 2.76 ppm, confirming that these two belong to the methylene groups of the phenethylamino moieties. Furthermore, since equatorial protons can be expected to show one strong geminal coupling and two smaller vicinal couplings, while axial protons are expected to exhibit two strong couplings (geminal and diaxial) and one smaller vicinal coupling, we could assign the broad doblets at 4.51 and 3.46 ppm, the broad triplet at 3.14 ppm and part of the ovelapped signal at 2.76 ppm to the C2'/C6'-H_{eq}, C3'/C5'-H_{eq}, C2'/C6'-H_{ax}, C3'/C5'-H_{ax} protons, respectively, of the piperazine system.

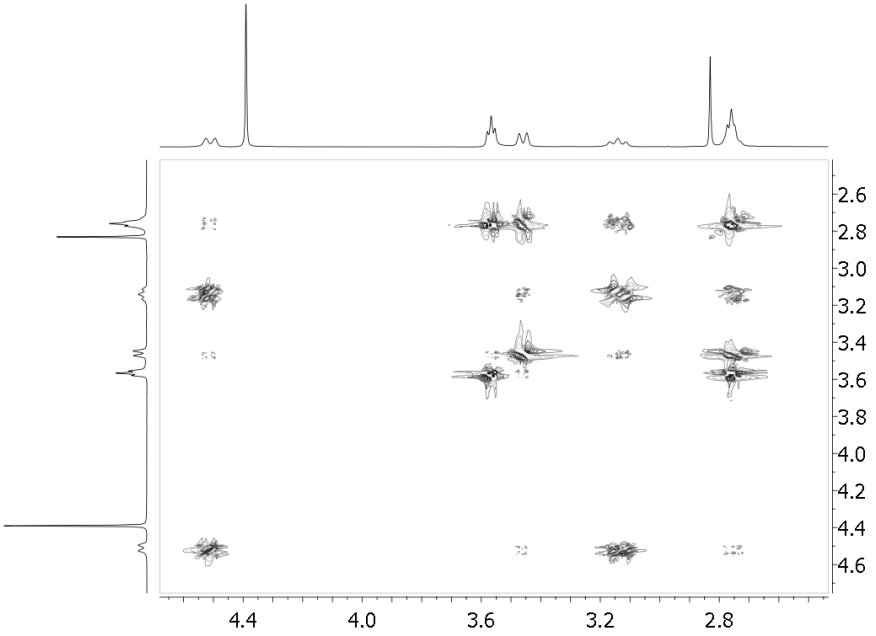

Figure 74. gDQCOSY spectrum of triazine **43** in ACN-d_3 (25 ºC).

3.2 Characterization of the dynamic equilibrium between triazine conformers.

To further characterize the conformational equilibrium between triazine rotamers, additional computational and NMR experiments were devised with the aim to determine the energetic barriers and relative rotamer populations for a representative compound. In particular, we focused on triazine **46** which was the most active TRPV1 blocker identified from this work, because knowing if one particular conformation could be determined as the most energetically favoured would be relevant to elaborate hypothesis about the biologically active conformation of this compound.

3.2.1 Theoretical study on the equilibrium between tris-aminosubstituted triazine rotamers.

Given the high flexibility of the substituents of the triazine ring of compound **46**, in order to reduce the computer time we decided to perform all the computational work on a simplified triazine model in which the substituents bound to the three amino groups were replaced by methyl groups. In this way, only two rotamers had to be considered (Figure 75).

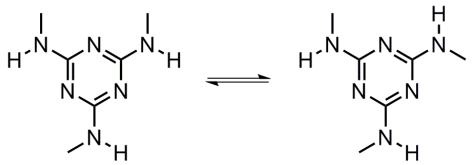

Figure 75: Rotamers of 2,4,6-tris(methylamino)-1,3,5-triazine.

Taking into account the piramidalisation of the nitrogen atoms during rotation,[124] and the fact that some rotations are degenerate because of symmetry, i.e. they go through the same transition state and/or conduct to the starting conformation, the complete conformational scheme for the interconversion between both rotamers is that shown in Figure 76a.

The structures of the two rotamers and of the transition states shown Figure 76a were calculated using Density Functional Theory methods (DFT). Thus, both minima and the four transition states were optimized at the B3LYP/6-31++G** level,[127-129] under implicit acetonitrile solvation conditions (the selection of this solvent was made because it was the one chosen to carry out further NMR experiments, see next section), using the software Jaguar[130] included in the Schrodinger Suite 2012.[130] Vibrational frequencies were calculated to characterize the nature of the determined stationary points as minima (no imaginary frequency) or transition states (one imaginary frequency), and the zero-point energies (ZPE) as well as the thermal and entropic corrections required to calculate Gibbs free energies were also determined. The standard Poisson-Boltzmann continuum solvation model implemented in Jaguar[131,132] was used to determine solution phase energies.

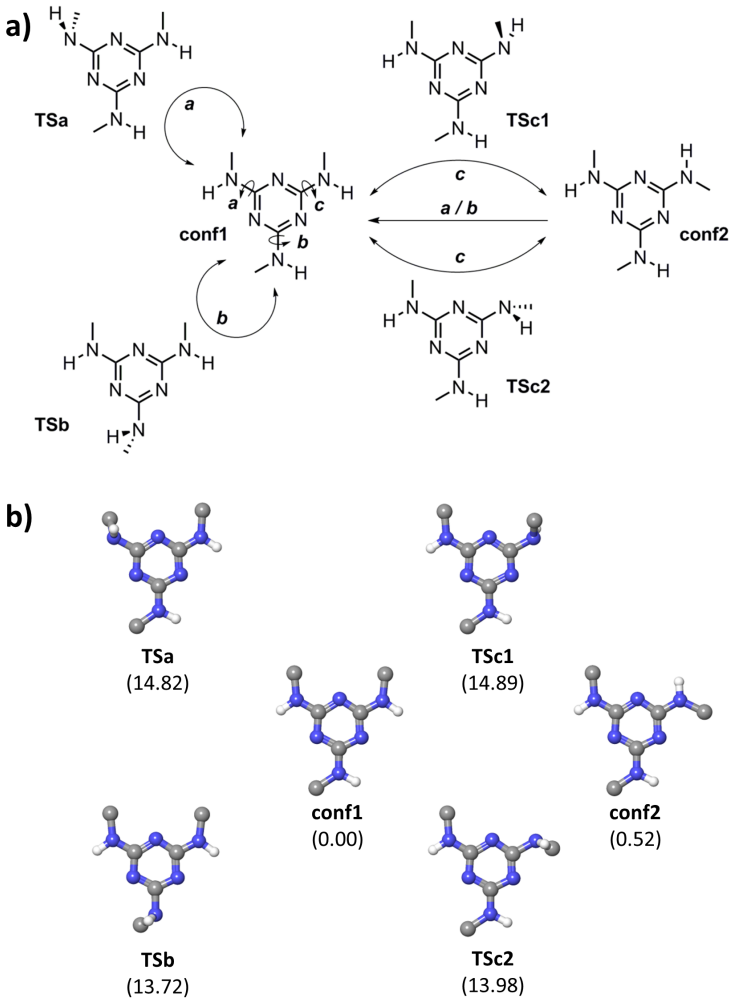

Figure 76. a) Conformational pathways for the interconversion between rotamers of 2,4,6-tris(methylamino)-1,3,5-triazine. b) Structures of minima and transition states calculated at the B3LYP/6-31++G** level under implicit acetonitrile solvation conditions, relative free energies in solution (ΔG^{sol}, kcal mol^{-1}) of each species are shown in parentheses.

Figure 76b shows the optimized structures and the relative free energies of the six stationary points determined, and Table 6 summarizes the thermodynamic parameters calculated for each of them.

The free energy difference between the two conformers, **conf1** and **conf2**, is small, slightly favoring the first one. The free energies of the four transition states are very similar, on average ΔG^{sol} = 14.4 ± 0.6 kcal mol^{-1}, indicating that for this triazine model there is almost no preference over one interconversion path or the others. These are in reasonable agreement with results obtained by NMR for the same model compound and related triazines in solvents like acetone-d_6 or DMF-d_6.[126]

Table 6. Gas phase energy (E^{gp}, hartrees), zero point energy (ZPE, kcal mol^{-1}), entropic (S, cal mol^{-1}) and enthalpic (H, kcal mol^{-1}) corrections at 298.15 K, acetonitrile solvation energy (E^{solv}, kcal mol^{-1}), total Gibbs free energy in solution (G^{sol}, hartrees), and relative free energy (ΔG^{sol}, kcal mol^{-1}), determined through density functional theory calculations at B3LYP/6-31++G** level for the stationary states determined along the conformational paths shown in Figure 76a.

	E^{gp}	ZPE	S	H	E^{solv}	G^{sol}	ΔG^{sol}
conf1	-564.464550	125.97	111.23	8.61	-15.56	-564.327721	0.00
conf2	-564.465058	125.98	111.25	8.61	-14.72	-564.326888	0.52
TSa	-564.438212	125.71	106.89	8.04	-17.72	-564.304106	14.82
TSb	-564.439030	125.73	107.13	8.05	-18.27	-564.305860	13.72
TSc1	-564.438847	125.74	106.57	8.00	-17.35	-564.303988	14.89
TSc2	-564.438669	125.68	107.70	8.08	-18.05	-564.305437	13.98

3.2.2 NMR study on the conformational equilibrium between rotamers of triazine 46.

Trying to extent the above theoretical study to a full triazine structure like **46** to predict the relative abundance of rotamers in solution and the energetic barriers for their interconversion would require an enormous amount of computing time. Therefore we decided to opt for a direct determination of these parameters using NMR methods. This study was carried out in collaboration with Dr. Ignacio Alfonso from our institute and most of the experiments described here were carried out on a 500 MHz NMR spectrometer equipped with a variable temperature accessory that allows to acquire spectra of samples at low temperature.

The line-shapes of NMR signals of nuclei that are involved in chemical exchange contain information on the rate constants of the exchange. Those processes occur with time scales comparable to the reciprocal of the frequency difference between the exchanging signals. One of the most common methods to evaluate the interconversion energy barrier is the determination of the temperature at which the NMR resonances of exchanging species coalesce. For a two equipopulated site exchange, the coalescence temperature (T_c, K) used in conjunction with the maximum peak separation in the low-temperature limit ($\Delta\nu, \mathrm{Hz}$) can be used in equations (*i*) and (*ii*) to evaluate the rate of conversion (k_c) and the activation energy of the exchange process ($\Delta G^{\ddagger}$).[133,134]

Equation (*i*) $$K_C = \frac{\pi\Delta\nu}{\sqrt{2}}$$

Equation (*ii*) $$\Delta G^{\ddagger} = RT_c \ln\left(\frac{\sqrt{2}k_B T_c}{h\pi\Delta\nu}\right) = RT_c\left[22.96 + \ln\left(\frac{T_c}{\Delta\nu}\right)\right]$$

K_B and h are the Boltzmann's and Planck's constants and eq. (*ii*) is derived from eq. (*i*) and Eyring's equation (*iii*).

Equation (*iii*) $$k = \frac{k_B T}{h} e^{-\frac{\Delta G^{\ddagger}}{RT}}$$

The ^{1}H-NMR spectrum of triazine **46** exhibited large differences in the chemical shift and shape of some signals when different solvents and temperatures were compared (Figure 77)

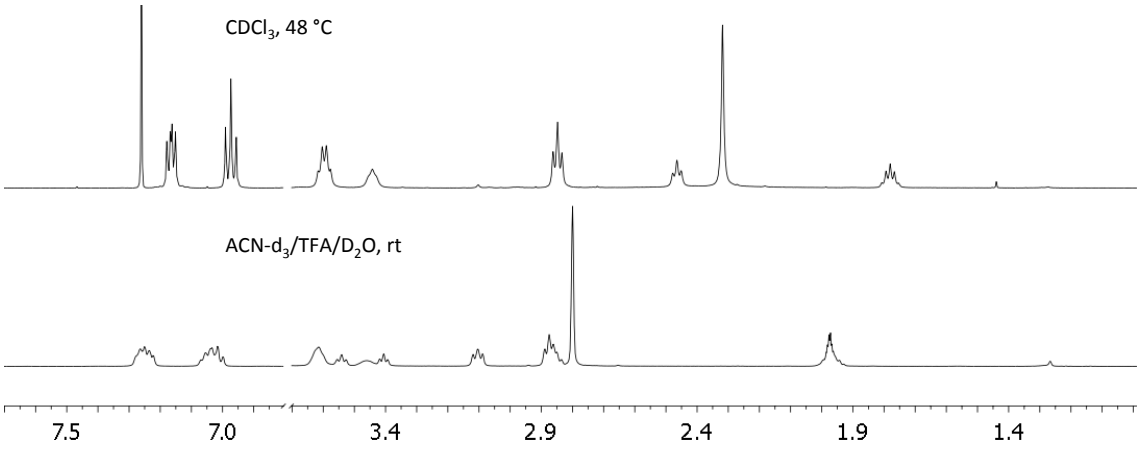

Figure 77: Comparison of the ^{1}H-NMR spectra of triazine **46** in two different solvents and temperatures.

Therefore, to perform the intended study, first, different deuterated solvents were tested to determine which was most appropriate in terms of solubility and stability under a range of temperatures, and for the observation of the exchange process. Using D_2O as representative of the vehicle in which biological experiments were performed was impossible due to solubility problems. Thus, spectra in ACN-d_3, ACN-d_3/D_2O (7 %) DMSO-d_6 and $CDCl_3$ were acquired at different temperatures (Figure 78).

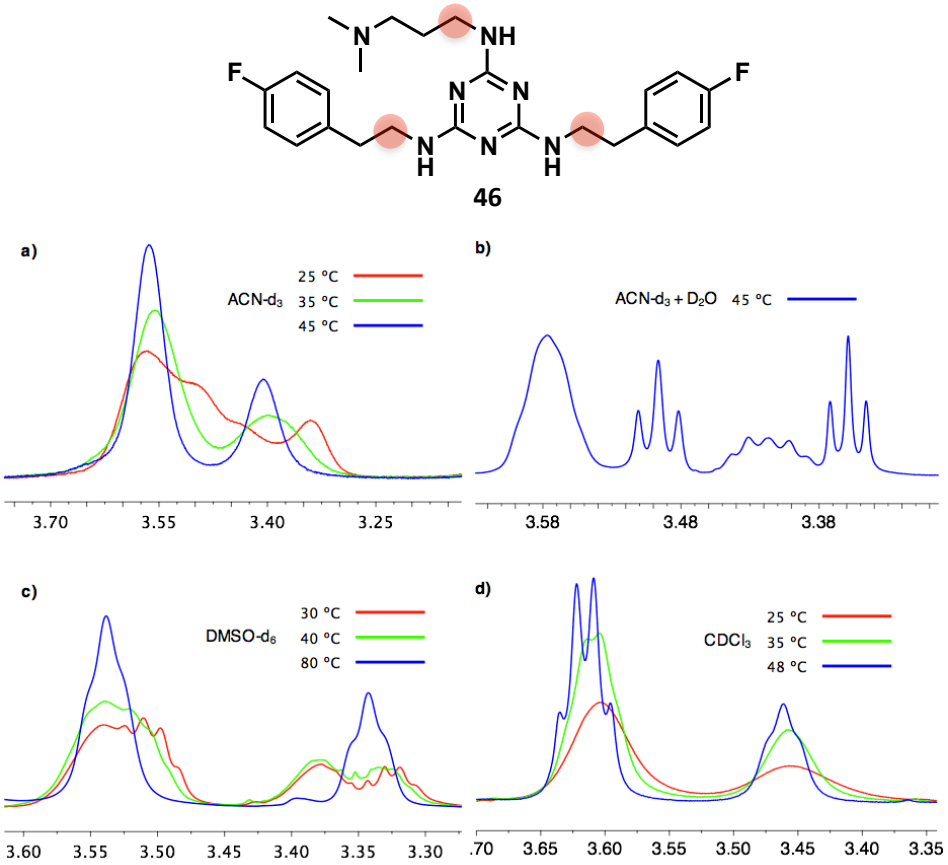

Figure 78. ^{1}H-NMR spectra of compound **46** in the region 3.30-3.70 ppm using different solvents and temperatures. The signals shown are those of amine-bound methylenes marked as red circles in the chemical structure.

The ^{1}H-NMR signals of the amine-bound methylenes closer to the triazine are those exhibiting higher anisochrony and exchange effects. Among the solvents assayed, $CDCl_3$ presents the less complex spectra even at low temperatures, achieving coalescence near 25 ºC. The mixture of ACN-d_3/D_2O shows a good separation of rotamer signals even at 45 ºC. This solvent mixture was the only one containing a protic solvent (D_2O), which suggests that hydrogen bonding with the solvent could increase the energy barrier of the transition between conformers, hampering conformer exchange. This seems to be confirmed by the fact that the spectra acquired in ACN-d_3 alone indicate a lower coalescence temperature, i.e. around 35 ºC. Finally, DMSO-d_6 was the solvent with higher coalescence temperature (> 80 ºC). This results in complex spectra at most temperatures, being the worst solvent to perform the desired NMR studies. Considering also that observation of the NH signals could provide additional information about the dynamic processes that we were interested on, it seemed that ACN-d_3 (without D_2O) was the solvent of choice (Figure 79).

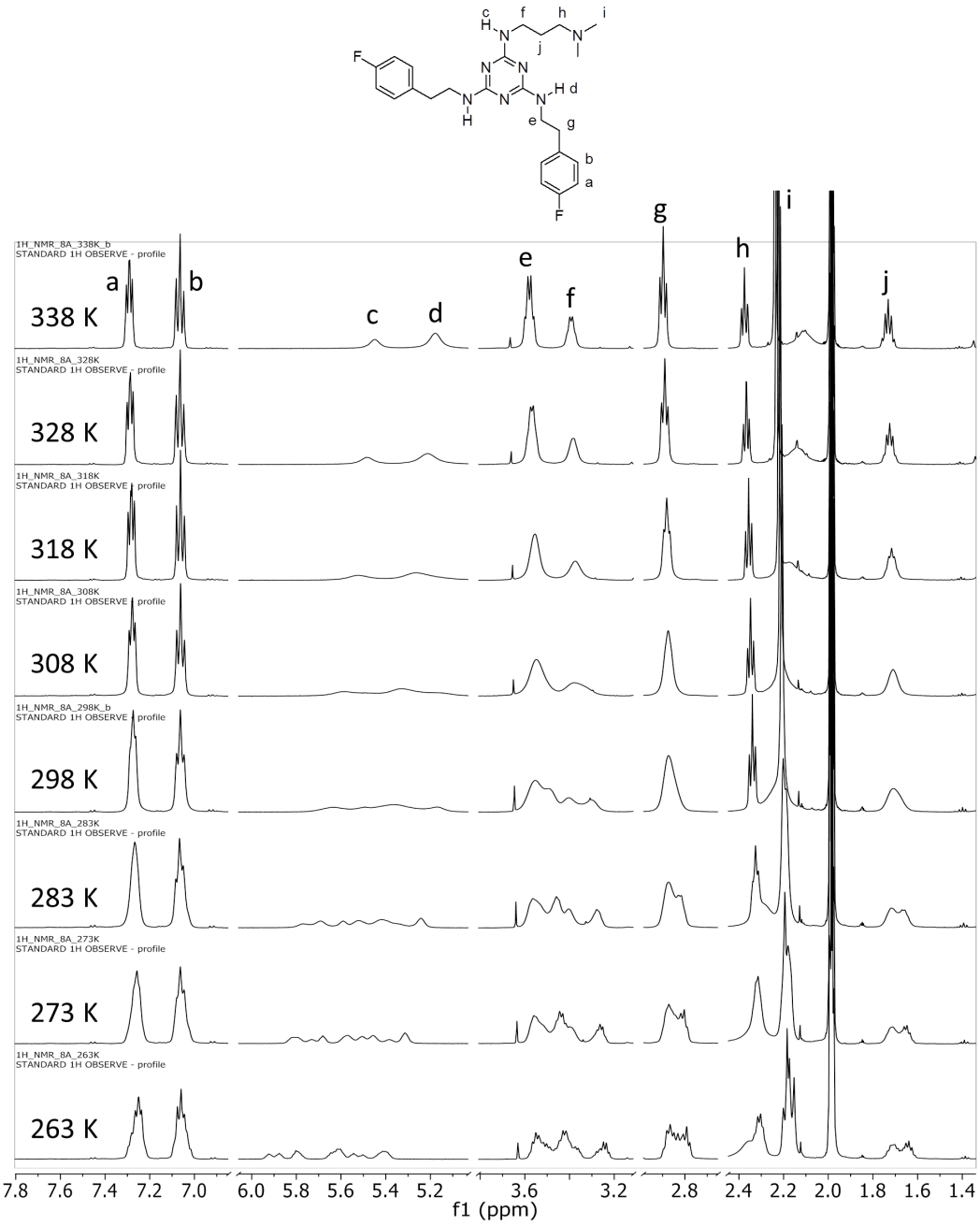

Figure 79. ^{1}H-NMR spectra (500 MHz) of triazine **46** in ACN-d_3 at temperatures from 65 (top) to -10 ºC (bottom).

Using Equation (ii) shown on page 89, an initial estimate of the energetic barrier for rotamer interconversion of triazine **46** could be obtained (Table 7). Looking at the different coalescing signals from the spectra shown in Figure 79, an estimated average $\Delta G^{\ddagger}$ value of around 14 kcal mol^{-1} could be calculated, in good agreement with the results from the theoretical prediction obtained with the triazine model. However, it is worth noting that the $\Delta G^{\ddagger}$ values shown in Table 7 should be taken only as a rough approximation because applying equation (*ii*) implies the assumption that there are only two species and a single equilibrium involved, while as previously stated there are four

possible rotamers for tris-aminosubstituted triazines and several equilibria that can be involved for their interconversion (see Figure 65c, pp.79).

Table 7. Estimation of the energy barrier ($\Delta G^{\ddagger}$) for the interconversion between rotamers of triazine **46** from the coalescence temperature (T_c) and maximum peak separation ($\Delta\boldsymbol{\nu}$) derived from spectra shown in Figure 79. Average $\Delta G^{\ddagger}$: 14.4 ± 0.6 kcal mol^{-1}.

$\Delta\nu$ (Hz)	T_c (ºK)	$\Delta G^{\ddagger}$ (kcal mol^{-1})
10.4	273.15	14.3
8.7	273.15	14.4
13.6	283.15	14.7
23.8	273.15	13.8
63.3	273.15	13.3
21.1	283.15	14.4
60.6	308.15	15.1
60.3	308.15	15.1
38.2	298.15	14.9

In order to determine the relative abundances of rotamers in solution we looked at groups of split signals with enough separation to obtain a good signal integration value for each one. At low temperature (i.e. -10 ºC, Figure 79), the NH signals showed a good separation between them (Figure 80a), however the number of peaks, some of them overlapped, was too high as to decide which correspond to each rotamer. On the other hand, the signal from the dimethylamino groups, revealed the presence of four different peaks that could be assigned to the four expected rotamers (Figure 80b). Using the Global Spectral Deconvolution fitting algorithm included in the Mnova Suite,[135] which can estimate the shape of each overlapped peak and its area, the relative abundance of each rotamer could be estimated. Three of them were approximately isopopulated while the abundance of the fourth was about half of the other three. Thus, an approximate 2:2:2:1 molar ratio between the four rotamers could be inferred under these experimental conditions.

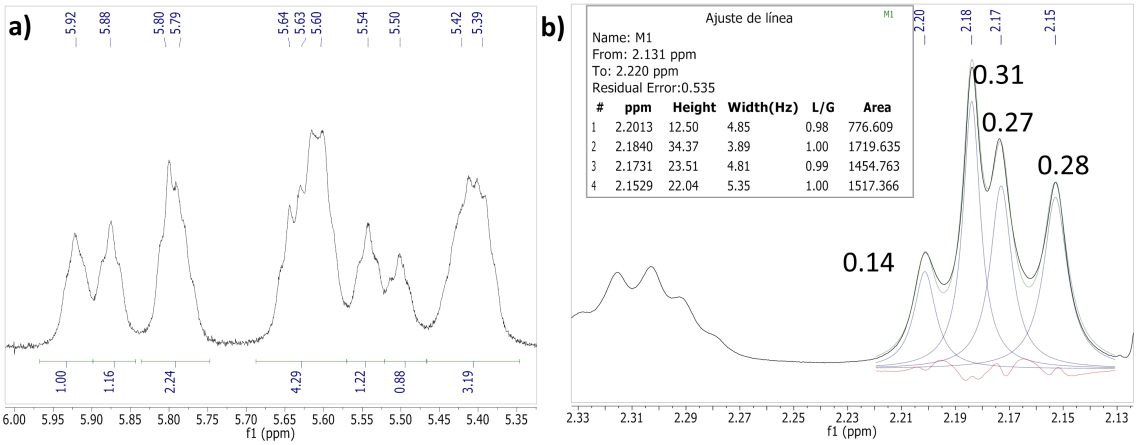

Figure 80. ^{1}H-NMR (500 MHz) of triazine **46** in ACN-d_3 at -10 ºC zoomed in the regions where the amine protons (a) and the dimethylamino protons (b) appear. The inlay table (b) shows values for the mathematical fitting using the Global Spectral Deconvolution algorithm of the Mnova software. Numbers over the peaks show the relative abundance ratio between them.

When exchange involves several not equipopulated species and several equilibria, more robust methodologies are required to get better estimates of the energy barriers. 2D-NMR techniques like 2D-Exchange Spectroscopy (2D-EXSY) can be used for that purpose.[136-139] The EXSY experiment uses the NOESY pulse sequence, however the mixing time is usually shorter since the exchange rate is normally faster than the cross-relaxation rate. Crosspeaks occur due to chemical exchanging protons if the right mixing time is chosen and they exhibit the same phase as the peaks from the diagonal. An optimal mixing time ensures that the evaluation of the kinetics of each transition is correct. On the other hand, if mixing time is too long, more than one equilibrium will take place and crosspeaks can be interconverted between them, giving an averaged information but no data of each individual process. A correct mixing time (t_{mix}) can be selected by measuring the evolution of the volume integrals of the diagonal and the crosspeaks (Figure 81) and choosing a value where enough signal built up is achieved without having reached the steady state.

The selected region of the NOESY spectrum to determine the best mixing time was that where the NH signals appear (6.1-5.2 ppm), since they were those that exhibit more exchange (Figure 81). Following the above criteria, it was concluded that a mixing time of 25 ms was the optimal value to obtain information about each equilibrium involved (Figure 82).

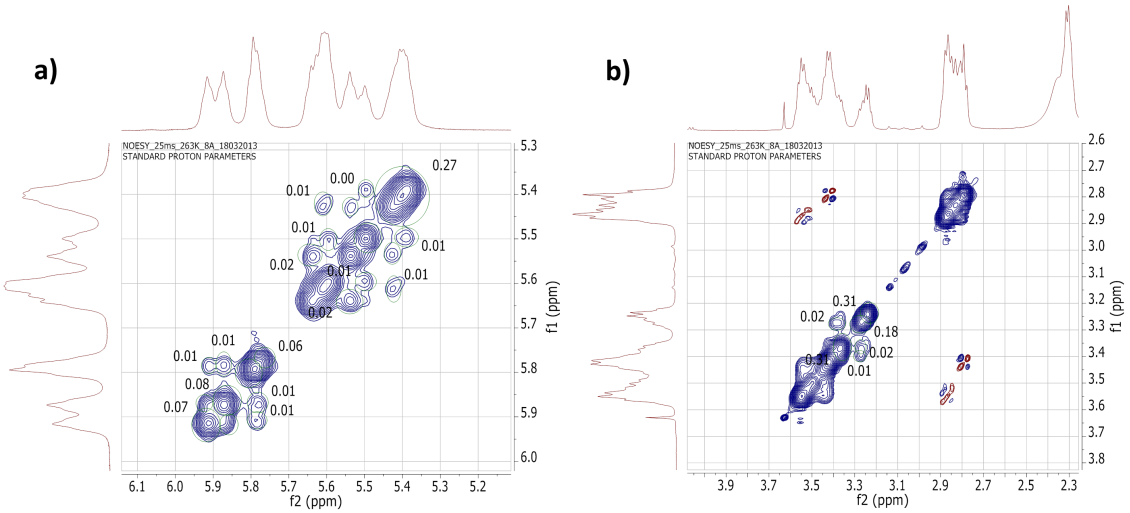

Figure 81. NOESY spectrum (500 MHz) of triazine **46** zoomed in the regions where the (a) NH and (b) aliphatic protons appear. The exchange signals and the diagonal are shown in blue. The spectrum was acquired in ACN-d_3 with a mixing time of 25 ms at -10 ºC.

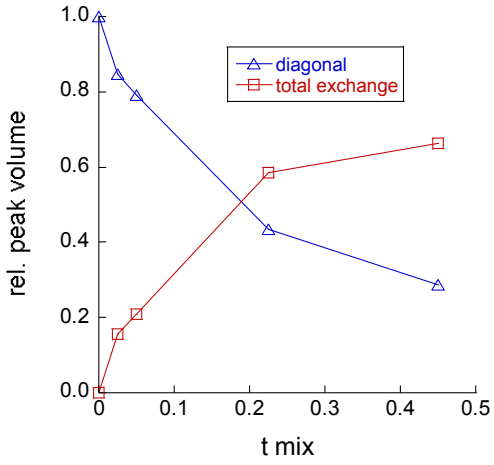

Figure 82. Evolution of volume integrals from the diagonal and the crosspeaks of NOESY spectra at mixing times (t_{mix}, s) of 25, 50, 225 and 450 ms. At t_{mix} > 225 ms a plateau is reached in the plot, indicating that shorter mixing times must be used in order to obtain kinetic exchange parameters of each intervening equilibrium.

The NOESY spectra acquired at t_{mix} = 25, 50, 225 and 450 ms and also a reference spectrum with t_{mix} = 0, all of these acquired and processed under identical conditions (temperature, number of scans, etc...), were used to generate a matrix with the volume integrals of the diagonal peaks and exchange crosspeaks (i.e. those with the same phase as the diagonal). These were used as input for the tool EXSYCalc,[140] which can calculate the magnetization exchange rates of the exchange equilibrium, related with the reaction rate constants, for systems with an arbitrary number of exchange sites, spins, populations and arbitrary longitudinal relaxation rates.

Considering that for triazine **46** there are four rotamers (A-D) in equilibrium, Table 8 summarizes the exchange rates calculated by EXSYCalc for the experiment at t_{mix} = 25 ms and the energy barriers derived from this experiment as well as the other experiments acquired at longer t_{mix} values, for comparison purposes.

Table 8. Exchange rates (*k*) from the EXSY experiment at t_{mix} = 25 ms and derived energy barriers ($\Delta G^{\ddagger}$) at different t_{mix} values. All exchange rates were calculated with the EXSYCalc software using data from NOESY spectra acquired at -10 ºC. Energy barriers were determined from Eyring's equation (*iii*, page 89).

	k **(s^{-1})**	**$\Delta G^{\ddagger}$ (kcal mol^{-1})**			
Process	**25 ms**	**25 ms**	**50 ms**	**225 ms**	**450 ms**
A → B	11.05	14.1	14.3	14.8	15.0
A → C	3.96	14.7	14.8	14.6	14.8
A → D	-0.52				
B → A	7.83	14.3	14.4	14.7	15.0
B → C	-0.38			14.7	15.2
B → D	3.98	14.7	15.1	14.8	15.0
C → A	2.45	14.9	14.9	14.7	14.7
C → B	-0.33			14.8	16.7
C → D	0.020	17.5	17.4	15.4	15.1
D → A	-0.60				16.3
D → B	6.52	14.4	14.7	15.2	15.4
D → C	0.038	17.1	16.9	15.3	15.4

Looking at the results from the experiment ran with t_{mix} = 25 ms, it appears that there are four calculated kinetic constants with small negative values which correspond to transformations (i.e. A ⇔ D and B ⇔ C) that are not taking place under the conditions of the experiment (there is no exchange between signals in the 2D-NOESY). Among the rest, most of the exchange processes occur with measurable rate constants between 2.5-11.0 s^{-1}, corresponding to activation energies between 14-15 kcal mol^{-1}, which again agree well with our previous estimations based on the theoretical calculations (see section 3.2.1). However, there are also two constants, i.e. those corresponding to the equilibrium C ⇔ D, which exhibit small positive values, corresponding to activation energies >17 kcal mol^{-1}. These results are consistent with

those obtained at t_{mix} = 50 ms, but at longer t_{mix} values it is apparent that some activation energies begin to diverge due to mixing of more than one process.

Altogether these results suggest that the number of conformational equilibria that are taking place is smaller than what was previously assumed (cf. Figure 65c, pp. 79), and that it can be represented by the scheme shown in Table 9. Based on the determined forward (k_i) and reverse (k_{-i}) rate constants for each equilibrium, an apparent equilibrium constant (K^{app}) can also be determined. Then, from these K^{app} values a 1.2 : 1.6 : 1.9 : 1.0 molar ratio for the mixture of conformers A : B : C : D could be estimated, which is in reasonable agreement with the ratios determined from fitting the methyl signals of the ^{1}H-NMR (Figure 80b, pp. 93).

Table 9. Exchange equilibria determined from 2D-EXSY experiments for triazine **46**: forward (k_i) and reverse (k_{-i}) rate constants and apparent equilibrium constants ($K^{app} = k_i/k_{-i}$).

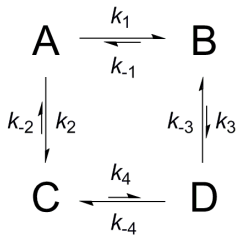

	k_i (s^{-1})	k_{-i} (s^{-1})	K^{app}
A → B	11.05	7.83	1.41
A → C	3.96	2.45	1.62
B → D	3.98	6.52	0.61
C → D	0.020	0.038	0.53

Thus, although based on these results it is not possible to assign rotamers A-D to any particular conformer structure, the conformational scheme shown in Figure 65cwould be reduced to a simpler one where, apparently, rotation *b* cannot take place (Figure 83a). Interestingly this would correspond to rotation of the dimethylaminopropyl moiety. It could be speculated that this could be due to the existence of an intramolecular hydrogen bond between the amino and the dimethylamino groups (Figure 83b), which would increase the sp^2 character of the amine nitrogen, thus stabilizing the planar conformation and increasing the energy barrier to rotation.

Concerning the relevance of these results for what might be occurring under biological conditions, while they confirm that under the NMR experimental conditions (acetonitrile solution at -10 ºC) there is little preference for any of the rotamers and all of them exist in equilibrium in solution, it is possible that this picture could change in water solution.

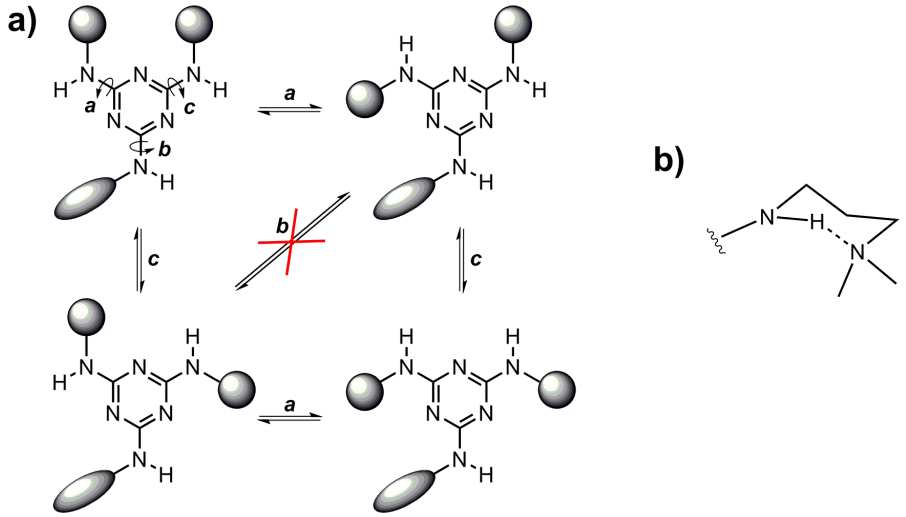

Figure 83. a) Conformational equilibria for triazine **46** based on the results of the EXSY NMR experiments. b) Postulated hydrogen-bond which could lead to an additional stabilization of the planar amine conformation.

However, it seems unlikely that the energy barriers to rotation could increase enough in aqueous media as to suppress some of the exchange processes. Indeed, water solvation might reduce the significance of the hydrogen bond interaction depicted in Figure 83b. Thus, it is plausible that these equilibria can also take place under biological conditions and that the thermally accessible energy barriers to rotation allow that the presence of a biological receptor could pull the equilibria towards one particular active conformation.